IOP Conf. Series: Materials Science and Engineering **301** (2018) 012002 doi:10.1088/1757-899X/301/1/012002

Solidification and Microstructure of Ni-Containing Al-Si-Cu Alloy

Li Fang, Luyang Ren, Xinyu Geng, Henry Hu*, Xueyuan Nie and Jimi Tjong

Department of Mechanical, Automotive & Materials Engineering, University of Windsor, Windsor, ON, Canada N9B 3P4
*Corresponding author email: huh@uwindsor.ca

Abstract. 2 wt. % nickel (Ni) addition was introduced into a conventional cast aluminum alloy A380. The influence of transition alloying element nickel on the solidification behavior of cast aluminum alloy A380 was investigated via thermal analyses based on temperature measurements recorded on cooling curves. The corresponding first and second derivatives of the cooling curves were derived to reveal the details of phase changes during solidification. The nucleation of the primary α-Al phase and eutectic phases were analyzed. The microstructure analyses by scanning electron microscopy (SEM) with energy dispersive X-ray spectroscopy (EDS) indicate that different types and amount of eutectic phases are present in the tested two alloys. The introduction of Ni forms the complex Ni-containing intermetallic phases with Cu and Al.

1. Introduction

Aluminum alloy A380 as a representative of hypoeutectic Al-Si-Cu alloy has moderate properties and relatively low cost which is one of the most widely used lightweight material. Although die cast A380 is a commonly used lightweight material in the automotive industry, the relatively low mechanical properties limits the material to sustain moderate mechanical loading application. From previous studies, transition alloying element nickel (Ni) is found to be effective element for improvement of mechanical properties of Al-Si alloy at elevated temperature [1-3]. Studies on the modification with nickel on the morphologies on aluminum alloys conclude that the presence of additional Nickel elements in the aluminum alloy system allows formation of complex intermetallic phases including Al_2Cu, Al_3Ni, Al_7Cu_4Ni, Al_9FeNi and $Al_5Cu_2Mg_8Si_6$ which are found effective to the enhancement of mechanical properties at elevated temperature [4-6].

While advanced Al casting technologies are emerging, the potential of conventional Al casting alloys needs to be further explored to maximize their engineering performance without significant increases in materials and manufacturing cost. Squeeze casting, also known as liquid metal forging, extrusion casting and pressure crystallization, is one of the advanced casting technology which is capable of eliminating casting defects such as gas and shrinkage porosity [7-9]. Moreover, the soundness of squeeze cast A380 as well as Ni-containing A380 enables thermal treatment for further improvement of mechanical properties. Hence, a scientific understanding of the solidification behavior of these alloys becomes essential for the establishment of correct thermal treatment processes.

However, most previous studies on aluminum alloys containing Ni addition were focused on the property evaluation and microstructure. Limited information on the effect of nickel content on solidification of squeeze cast Al-Si-Cu alloys is available in the open literature. The objective of this study is to investigate the effect of nickel (Ni) addition on the solidification behavior and microstructure development of aluminum alloy A380. Thus, computer based thermal analyses was utilized to study the occurrence of nucleation during solidification and grain microstructure.

2. Experimental Procedures

2.1. Materials and Processing

The base material selected for this study is the conventional aluminum alloy A380 with its chemical composition listed in Table 1. Predetermined amount of A380 alloy and Al-20 wt. % Ni master alloy were melt and mixed in an electric resistance furnace to achieve the desired compositions which were verified by an Inductively-Coupled Plasma Atomic Emission Spectrometer based on ASTM E1479-99. The melt was kept at 730±10°C for 30 minutes for the completion of homogenization and modification under the protective gas of nitrogen, and then the melt temperature was decreased to 700°C for pouring.

Table 1. Chemical composition of A380 (wt. %)

Alloys	Si	Cu	Fe	Mn	Mg	Zn	Ni
A380	8.5	3.5	1.3	0.5	0.10	3.0	0.50
2.0Ni/A380	8.5	3.5	1.3	0.5	0.10	3.0	2.5

2.2. Thermal Analysis

For each thermal analysis, about 300 grams of melt sample were taken from the well-stirred alloys at into a small crucible. A chromel-alumel (K-type) thermocouple protected by a thin steel sheath was positioned at a distance of 0.02 m from the bottom of the crucible center, and was connected to a computer-based data acquisition system to measure the temperature variation. In thermal analysis, the temperature of the solidifying alloy samples was recorded by the data acquisition system at a regular interval of 100 ms as they cooled from the completely liquid state, through the solidification range, to become fully solid. The acquired temperature (T) vs. time (t) data from 650 °C to 450 °C were processed, and cooling curves (T vs. t) were plotted using the Microsoft Excel spreadsheet software. The corresponding first and second derivative curves (dT/dt and d^2T/dt^2) were also derived and plotted to reveal detailed characteristics of solidification that cannot be detected on the cooling curves alone. Several duplicate runs on each melt were conducted to ensure an uncertainty of ±0.1%.

2.3. Microstructural Analysis

Specimens were sectioned, mounted, and polished from the center of the squeeze cast cylindrical coupons, and prepared following the standard metallographic procedures. A Buehler (Lake Bluff, IL) optical image analyzer 2002 system was used to observe primary characteristics of the specimens. The detailed features of the microstructure were also characterized at high magnifications by a scanning electron microscope (SEM), i.e., Hitachi Tabletop Microscope TM3000. To maximize composition reading of the energy dispersive spectroscopy (EDS) data, an etchant of 0.1 % NaOH solution was applied to polished specimens for microscopic examination.

3. Results and Discussion

Figure 1. represents a cooling curve recorded during solidification of the A380 casting alloy along with the corresponding first derivative and second derivative curves. The presence of peaks on a dT/dt derivative curve indicates that a phase transformation occurs due to releasing latent heat at an increased rate. The peaks on a second derivative curve are considered as the accurate indicator of nucleation temperatures, when the d^2T/dt^2 curve varies considerably [10]. The temperature at which the very first crystal nucleates, stabilizes and starts to grow can be determined. Furthermore, the peak on the second derivative curve indicates a minimum temperature, at which the nucleated crystals have grown in such a way that the liberated latent heat of fusion balances the heat extracted from the samples. Examination of the cooling curve illustrated in Figure 1 manifests four distinguished stages during the solidification process of A380 alloy. The nucleation of primary aluminum α-phase happened in stage I, from which the non-equilibrium liquid temperature was recorded as 574.03-577.48 °C. Stage II at 569.76°C is the nucleation of Al_5FeSi phase, which has no obvious undercooling detected. Stage III is the occurrence of the eutectic reaction, i.e., $L \rightarrow Al\ (\alpha) + Si\ (\beta)$,

where the non-equilibrium solidus temperature was determined as 558.48°C with an observed undercooling phenomena of 1.09 °C. At stage IV, the intermetallic phases precipitated at 490.03 °C, i.e., L → Al (α) + Si(β) + Al_2Cu(θ). No undercooling phenomena were observed for the solidification of the intermetallic phase. The solidification rate of the A380 alloy is 10.7 °C/min, which was calculated by the division of the temperature difference between Stages I and IV with the corresponding time interval. The non-equilibrium phase change temperatures are in good agreement with the data existing in the literature [11].

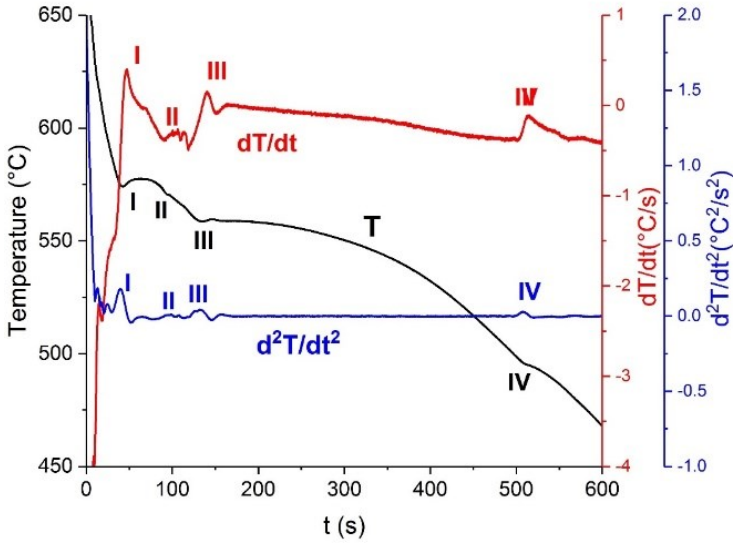

Figure 1. The typical cooling curve of the as-cast A380 alloy and its corresponding first and second derivative curves.

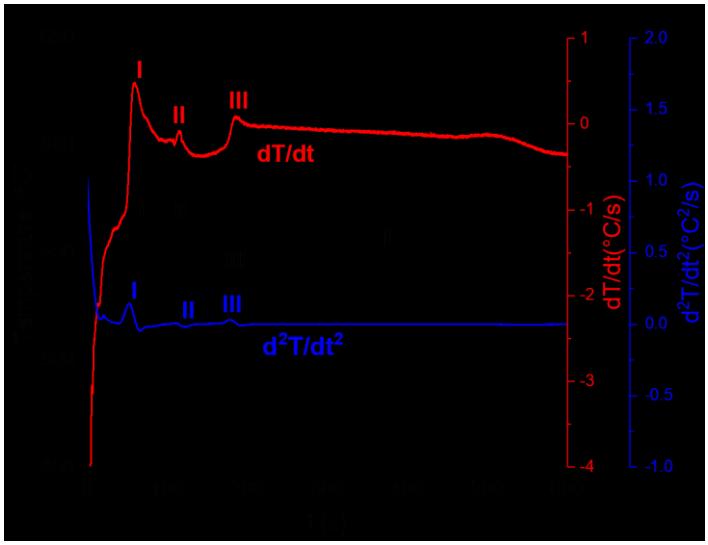

Figure 2. The typical cooling curve of the as-cast A380+2%Ni alloy and its first and second derivative curves.

The typical cooling curve of A380 alloyed with 2.0 wt. % Ni addition is given in Figure 2, which reveals a three-stage solidification behavior. The formation of primary α-phase begins at 576.28°C in stage I. Moving to the second stage, a very interesting feature observed from A380+2%Ni alloy cooling curve is that the second stage of the solidification takes place at temperature of 575.96°C, which is even higher (5.7 °C) than the temperature of the first stage present during the solidification of A380. The reason for such phenomenon might be related to the formation of Ni-containing Al-Cu

phase. It has been reported [12] that, during the equilibrium solidification of an Al-Cu- Ni alloy, a ternary phase $NiCu_2Al_5$ formed around 585 °C. Stage three of A380+2%Ni cooling curve is also observed which begins at 554.23°C. Based on the cooling curves depicted in Figures 1 and 2, a reduction of 4.25 °C is present at stage III because the addition of 2%Ni into the A380 alloy could lead to a ternary reaction, L => (Al) + Al_2Cu + $NiCu_2Al_5$. Although the evident appearance of stage III suggests that it should be considered as the last stage of the solidification process for the A380+2%Ni alloy, a slight change of the slope of the first derivation curve is present at around 525 °C. But, it is too weak to be regarded as a peak. This observation implies that Al_2Cu phase might form at the end of the A380+2%Ni solidification. However, the amount of the Al_2Cu phase is insufficient to generate adequate latent heat. Considering that the solidification ends at the formation of the last Al_2Cu phase, the solidification rate of the A380+2%Ni alloy is only 6.5 °C /min, which is lower than that of the A380.

Figure 3 shows the microstructure of the etched A380 and A380+2%Ni alloys revealed by optical microscopy. Their microstructures mainly consist of the primary α-Al dendrites and eutectic phases surrounding their boundaries. The sizes of the primary α-Al dendrites are similar for both conventional and Ni-containing A380 alloys. The comparison of Figure 3(a) and (b) manifests that the Ni addition has a limited influence on the morphology and size of the primary α-Al phase. Eutectic silicon phase is identified as long needle shape which is in deep grey color. Using ImageJ, micrographs were converted to binary black and white images, with black areas representing intermetallics, while light areas representing primary α-Al and eutectic silicon phases. Following conversion, the software automatically calculated area fractions of black and white areas. Figure 4 presents the converted micrographs highlighting the presence of intermetallics in the observed alloys represented by the black area. By comparing the Ni-containing A380 alloy with the conventional base alloy, the image analysis reveals that the area percentage of the intermetallic phases increases with additional Ni content. Figure 4 shows the variation of the volume fraction of intermetallic with the 2% Ni content addition. The area percentage of the intermetallic phases in the conventional A380 alloy is measured to be 4.3% and 10.2% for A380 and A380+2%Ni alloys respectively. This observation can be concluded as that with additional Ni content in the base A380 alloy, the size and amount of Ni-containing intermetallic dramatically increase. Ni as a transit element, forms intermatallics with both Al-Cu and Al-Fe phase and trend to aggregate to bigger intermetallic. Figure 5 presents the SEM micrographs and the EDS patterns evidently showing the presence of (a) Al_2Cu phase in the A380 and (b) Ni-containing Al-Cu phase in the A380+2%Ni alloys. The presence of the Ni-containing Al-Cu phase should be responsible for the evident appearance of the second stage on the dT/dt derivative curve of the A380+2%Ni alloy. Compared with that of the base A380 alloy, the relatively low solidification rate appeared during the solidification of the A380+2%Ni alloy should be attributed to the high latent heat release resulting from the formation of a large amount of the ternary phase ($NiCu_2Al_5$) might result in the the Ni-containing Al-Cu phase.

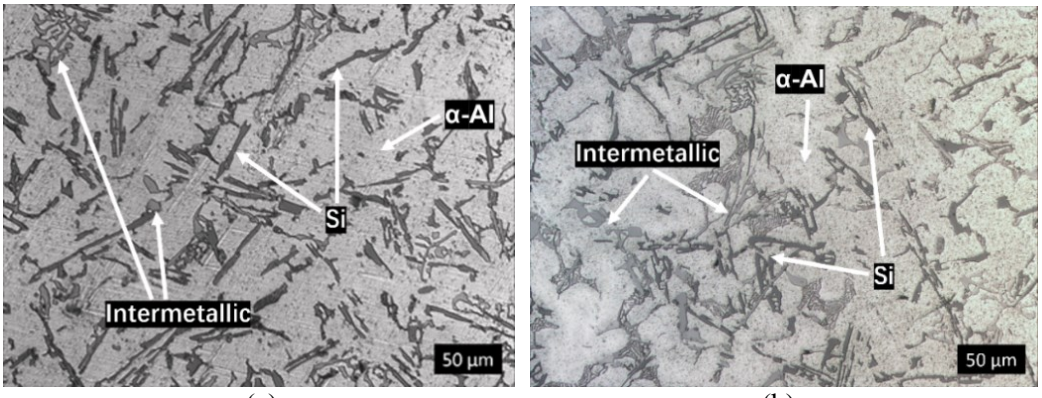

(a) (b)

Figure 3. Optical micrographs showing microstructures of the squeeze cast (a) A380 alloys and (b) A380+2%Ni alloy.

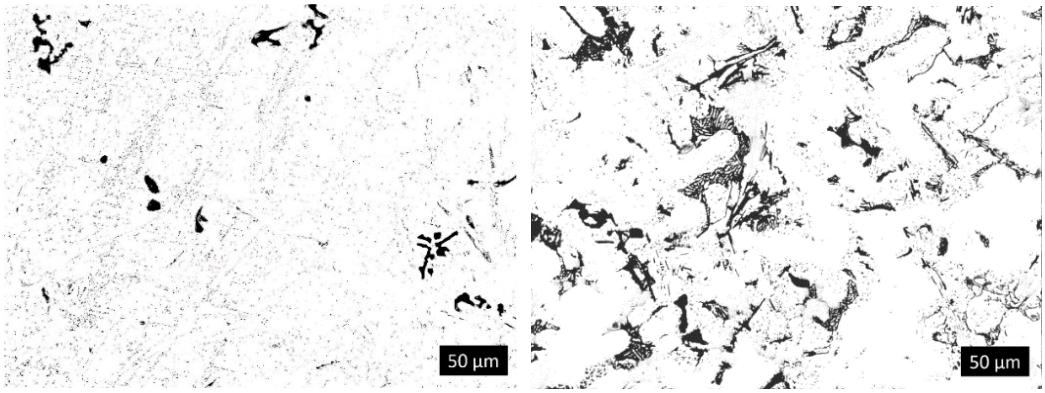

(a) (b)

Figure 4. Micrographs in binary black and white images showing intermetallic contents in squeeze cast (a) A380 and (b) A380+2%Ni alloys.

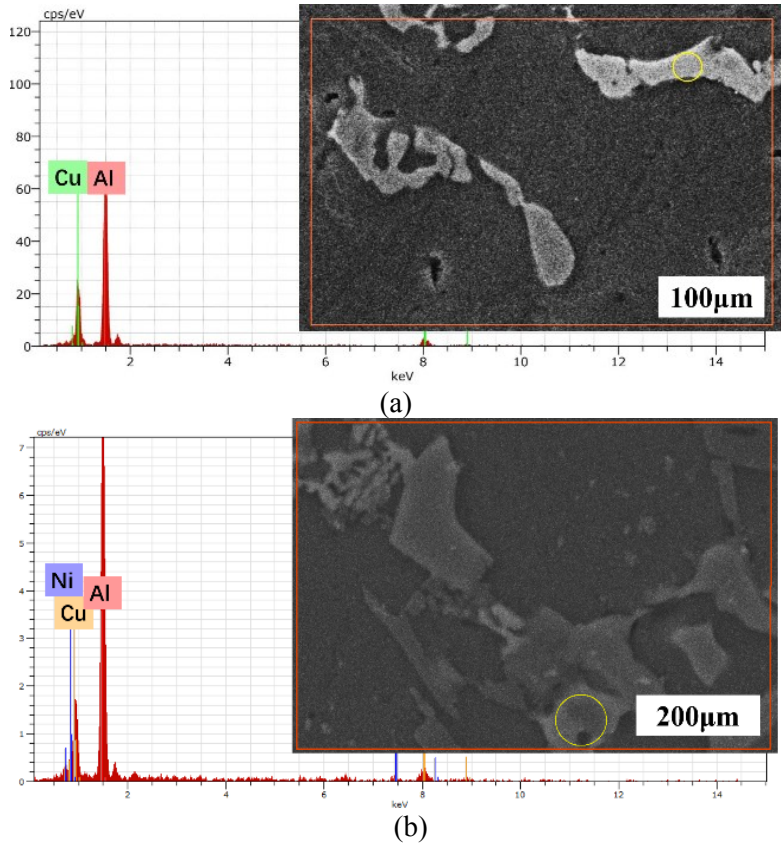

Figure 5. SEM micrographs showing the presence of (a) Al_2Cu phase in the A380 and (b) Ni-containing Al-Cu phase in the A380+2%Ni alloys.

4. Conclusions

The solidification behaviors of the conventional A380 and A380+2%Ni alloys are investigated by the thermal analysis. The observation of the high eutectic temperatures of imtermetallics on the cooling curve of the A380+2%Ni alloy implies the Ni addition promotes the formation of Ni-containing ternary phases which are absent in the base A380 alloy. The release of the latent heat by the Ni-containing ternary phase slows down the solidification process of the A380+2%Ni alloy. The detection of the Ni-containing ternary phase in large quantity present in the microstructure of the A380+2%Ni alloy supports the results of the thermal analyses. The determined phase change temperatures could be used to guide the establishment of thermal treatment procedures for the

A380+2%Ni alloy.

5. Acknowledgments

The authors would like to thank the Natural Sciences and Engineering Research Council of Canada (NSERC), Ford (Canada) and the University of Windsor for supporting this work.

6. References

[1] Wang L, Makhlouf M and Apelian D 2013 *Int. Mater. Rev.* **40(6)** 221
[2] Cho Y H, Joo D H, Kim C H and Lee H C 2006 *Mat. Sci. Forum* **519** 461
[3] Rajaram G, Kumaran S and Rao T S, 2011 *Mater. Chem. Phys.* **128(1)** 62
[4] Chen C-L, Richter A and Thomson R C 2010 *Intermetallics* **18(4)** 499
[5] Li Y, Yang Y, Wu Y, Wang L, and Liu X 2010 *Mat. Sci. Eng.* **A 527(26)** 7132
[6] Yang Y, Yu K, Li Y, Zhao D and Liu X 2012 *Materials & Design*. **33** 220
[7] Niu XP, Hu B H, Pinwill I and Li H 2000 *JMPT* **105(1)** 119
[8] Buffière JY, Savelli S Jouneau P H, Maire E and Fougeres R 2001 *Mat. Sci. Eng.* **A 316(1)** 115
[9] Chang Q, Chen C, Zhang S, Schwam D and Wallace J 2010 *Int. J. Cast Met. Res.* **23(1)** 30
[10] Sparkman D 1994 *In Ninety-Eighth Annual Meeting of AFS* p.229
[11] Hu XP, Fang L, Zhou JX, Zhang XZ, Hu H 2017 *China Foundry* **14(2)** 98
[12] Prince A, Kumar KH 1991, *Ternary alloys* **4** 597